EPTT 2024
Escola de Primavera de Transição e Turbulência

ABCM
Associação Brasileira de Engenharia e Ciências Mecânicas

EPTT-2024-XXXX
AIRCRAFT THERMAL MANAGEMENT: CFD ANALYSIS OF THE WING AS A SURFACE HEAT EXCHANGER

Lucas Silva Tazitu
Edemar Morsch Filho
São Paulo State University (UNESP)
School of Engineering, São João da Boa Vista
lucas.tazitu@unesp.br
edemar.filho@unesp.br

Abstract. *This study explores the feasibility of using fuel as working fluid in a surface heat exchanger based on the Boeing wing's geometry of 777-300ER. Through Computational Fluid Dynamics (CFD) simulations, two geometric configurations—parallel and serpentine—were evaluated under various operational conditions, including aircraft on the ground (AOG) and in cruise flight. The results indicate that the serpentine configuration achieves higher heat exchange rates, but requires higher inlet pressures. Conversely, the parallel configuration, while less effective in heat exchange, offers a simpler and potentially lighter solution. Higher mass flow rates were found to enhance heat transfer but reduced the cooling efficiency due to decreased fuel residence time in the heat exchanger.*

Keywords: *Aircraft thermal management, Heat exchanger, CFD simulation, Fuel cooling system*

1. INTRODUCTION

In order to make aviation more sustainable, aircraft electrification has become one of the most widely adopted alternatives by manufacturers. The three main classes of electrification are More Electric Aircraft (MEA), hybrid aircraft, and fully electric aircraft. These categories represent a progressive evolution toward more efficient and extensive use of electrical energy in aviation, each with its own distinct advantages and challenges (Schwab *et al.*, 2021).

The electrification of aircraft, the implementation of advanced electrical systems, and the miniaturization of their components create significant challenges for thermal management. Therefore, it is necessary to develop specialized systems for heat dissipation and thermal management to ensure the efficient and safe operation of these systems. A strategy often adopted in the military sector involves using the aircraft's own fuel as a coolant for internal systems (Gray and Shayeson, 1973). While this practice is common in that context, it is not yet widely employed in general aviation for thermal management.

As the number of electrical systems in hybrid aircraft increases, so does the heat generation, making thermal management even more crucial. Utilizing the fuel as a coolant represents a potential solution to address the thermal challenges associated with the growing number of electrical systems on board. Considering that fuel tanks remain located in the wings and that the fuel can also be used as a coolant, a strategic approach is the installation of a heat exchanger at the wing. This efficiently leverages the existing infrastructure in the aircraft to enhance thermal management, contributing to more effective thermal performance and an efficient operation throughout all phases of flight.

The main objective of this study is to analyze, through Computational Fluid Dynamics (CFD) simulations, the feasibility of a surface heat exchanger integrated into the aircraft's fuel flow. This heat exchanger is located between the wing surface and the fuel tank, with the purpose of dissipating heat generated by the aircraft's electrical systems.

2. METHODOLOGY

This study used the right main tank of the Boeing 777-300ER as a reference and JET-A fuel. The geometric model adopted simplifications to achieve a viable and efficient representation of the system, as shown in Figure 1.

The heat from generic sources on the aircraft is transferred to the fuel, which flows through ducts located between the upper wing surface and the top of the tank. Twenty equally spaced ducts of the same height and thickness were modeled, made from the same material as the fuel tank, crossing the wing's root until the wing's tip. The heat exchanger geometry was designed in Ansys SpaceClaim 2022 R2 using the contour of two surfaces, corresponding to the aircraft's upper

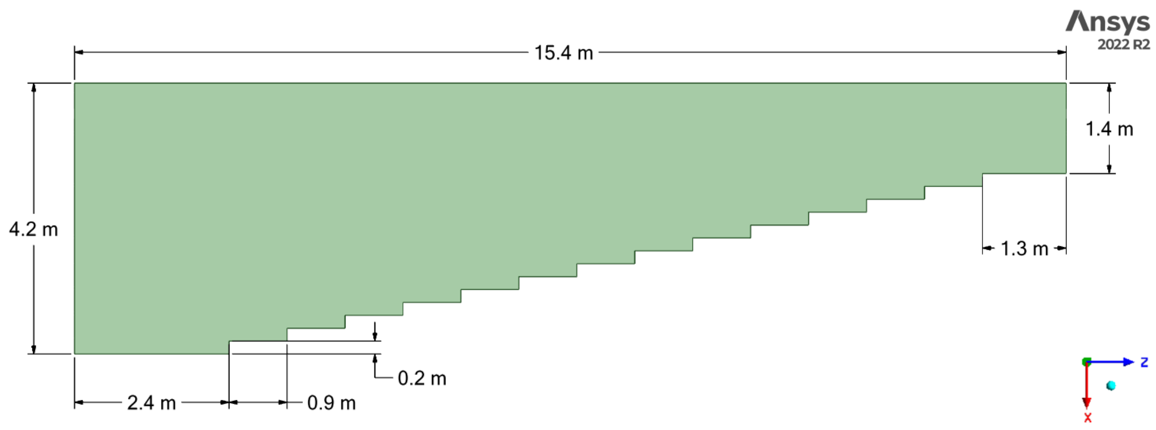

(a) Upper View.

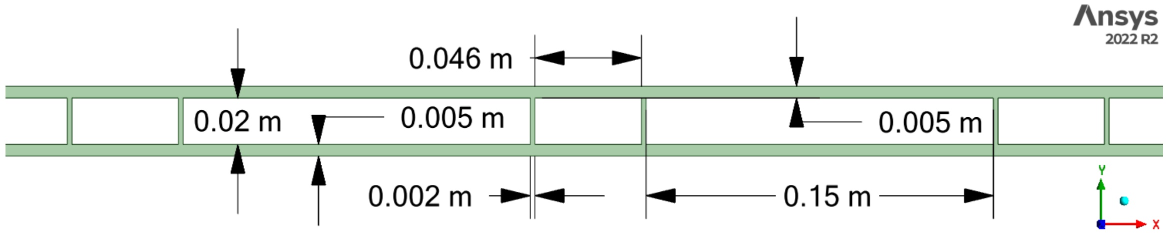

(b) Side View.

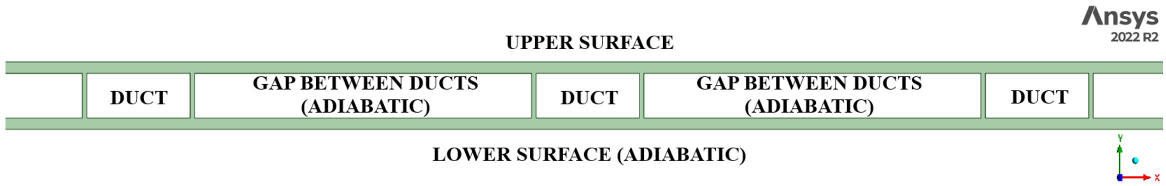

(c) Parts of the heat exchanger.

Figure 1: Heat exchanger geometry

surface and the fuel tank (Figure 1c). Between these surfaces, ducts were installed to allow the refrigerant fluid to flow. The entire solid domain was modeled as a single piece, made from 5052 aluminum alloy.

The geometric model was reproduced in Ansys ICEM CFD, version 2022 R2, to generate the mesh for the heat exchanger. Individual meshes were generated for the solid surface and the flow ducts, through which the fuel will flow. The mesh generation consisted of hexahedral models, and the quality of the elements were evaluated using a mesh metric in ICEM CFD.

The simulations were conducted using Ansys CFX, version 2022 R2. The software configuration considered steady-state flow and incompressible fluid. The k-ϵ turbulence model was chosen for the simulation due to its versatility, accuracy, and low computational cost. The k-ϵ turbulence model is more accurate in regions where the turbulent flow is fully developed but is not suitable for regions close to the walls. To accurately represent the flow near the wall, wall functions are employed to meet the specific physical requirements of this region. Using wall functions eliminates the need to resolve the boundary layer directly, as the equations are formulated to empirically capture the behavior of the flow near the wall. It is important to note that wall functions are used in this study because the simulation's objective is not related to wall forces. The wall function used in this study is based on the parameter y^+. For the wall function to be valid, y^+ was kept between 30 and 300; a value too low invalidates the model, while a value too high does not adequately resolve the boundary layer (Murad, 2020).

2.1 BOUNDARY CONDITIONS

The fuel will flow through the twenty ducts of the heat exchanger, and the boundary condition for the inlet of these ducts consists of a flow determined by the mass flow rate ($\dot{m}$) in a subsonic regime. The boundary condition for the outlet is determined by the average static pressure of the outlet. In this context, the relative pressure is zero, meaning that the fluid exits the system at 1 atm.

Heat transfer by convection occurs on the upper plate of the solid geometry, representing the contact of the flow with the upper surface of the aircraft wing. Due to the greater influence of forced convection effects on the upper surface, the gaps between the ducts and the lower plate of the solid, which represents the fuel tank, are considered adiabatic (Kellermann *et al.*, 2020). No angle of attack relative to the flow was considered.

A fluid-solid interface was created to preserve the flux of thermal energy, with a no-slip wall condition, and a smooth surface.

2.2 MATERIALS PROPERTIES

The properties of the International Standard Atmosphere (ISA) were used as a reference for the air properties in cruise flight, while the historical atmospheric data from São Paulo-Guarulhos International Airport was used for the aircraft on the ground (AOG) (World Weather Online, 2024). The properties of the fuel used were based on JET-A (Bruno *et al.*, 2006). The material chosen for the solid geometry is aluminum alloy Al 5052, known for its flexibility and high resistance to fatigue and corrosion.

2.3 CONVECTION HEAT TRANSFER

The local convective heat transfer coefficient at a position x (h_x) can be obtained through the local Nusselt number, defined as (Ghajar and Yunus A. Cengel, 2014):

- Laminar flow for Prandtl numbers Pr>0.6 and Reynolds numbers Re_x<500,000:

$$Nu = 0.332 Re_x^{0.5} Pr^{1/3} \tag{1}$$

- Turbulent flow for $0.6 \leq Pr \leq 60$ and $500,000 \leq Re_x \leq 10^7$:

$$Nu = 0.0296 Re_x^{0.8} Pr^{1/3} \tag{2}$$

Due to the high velocities encountered on the upper surface, compressibility effects can be significant depending on the aircraft's operating conditions. However, these correlations assume incompressible flow to simplify the analyses.

Therefore, forced convection heat transfer can be either laminar or turbulent, with the transition occurring at $Re_x > 500,000$.

Based on the investigated aircraft operation types, it is possible to calculate the local convective heat transfer coefficient along the upper surface of the wing, considering the maximum lateral length of 4.2 m (x-axis). The simulations for the AOG cases, shown in Figure 2a, incorporated both types of forced convection, where the transition from laminar to turbulent flow can be observed at 2.1 m. For cruise flight cases, shown in Figure 2b, only turbulent forced convection was considered, and its magnitude is significantly higher than in the AOG cases. It is important to note that Figure 2 use different scales to facilitate the visualization and understanding of the presented data.

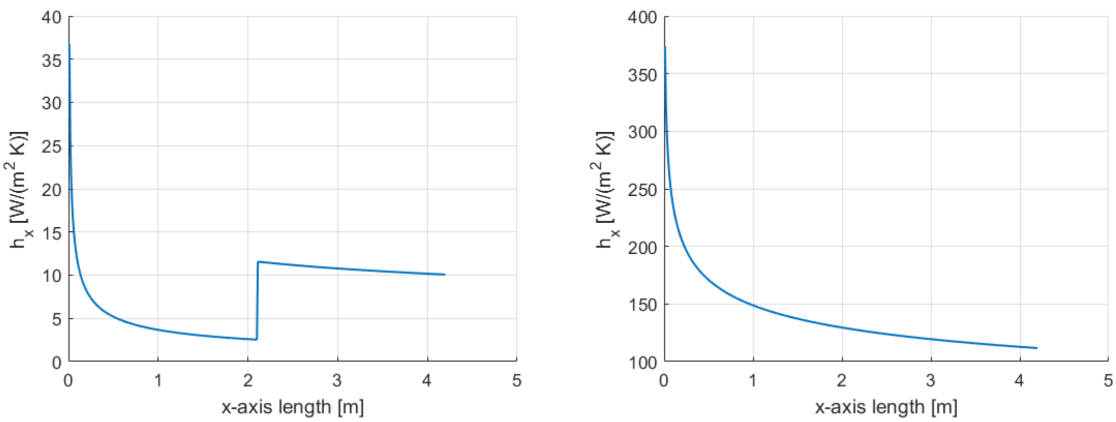

(a) h_x: Aircraft on Ground (b) h_x: Cruise flight

Figure 2: Convection heat transfer coefficient.

2.4 CASE STUDIES

Regarding the aircraft operation, two cases will be studied to investigate the influence of altitude, temperature, and flow velocity on the heat exchanger. The first type of operation is for the aircraft on the ground, using São Paulo-Guarulhos International Airport as a reference. The second type of operation considers the aircraft flying in a cruise flight (Cruise).The flow velocity is 3.64 m/s for the AOG operation and 249.09 m/s for the cruise flight cases.

To evaluate the effect of geometry on the heat exchanger, two configurations were proposed: one with parallel fuel flow through the ducts, independently along the wingspan, and another with fuel flowing in series through the ducts, forming a serpentine-shaped heat exchange system. To investigate the effect of mass flow rate ($\dot{m}$) in the simulation, $\dot{m}$ values of 1 kg/s and 10 kg/s were considered. The coolant liquid temperature (T_{fuel}) at the inlet of the heat exchanger was fixed at 350 K for all cases studied in this work.

Based on this information, eight simulations were proposed, covering a variety of operations, geometries and mass flow rates, as shown in Table 1.

Table 1: Simulations cases and conditions.

Case	Type of Operation	Geometry	$\dot{m}$ $[kg/s]$	T_{fuel} $[K]$
AOG-P-10	AOG	P (Parallel)	10	350
AOG-S-10	AOG	S (Serpentine)	10	350
AOG-P-1	AOG	P (Parallel)	1	350
AOG-S-1	AOG	S (Serpentine)	1	350
Cruise-P-10	Cruise	P (Parallel)	10	350
Cruise-S-10	Cruise	S (Serpentine)	10	350
Cruise-P-1	Cruise	P (Parallel)	1	350
Cruise-S-1	Cruise	S (Serpentine)	1	350

Each case will be identified by a sequential nomenclature indicating its type of operation, geometry, and fuel flow, e.g., AOG-P-10 is for aircraft on the ground with a parallel geometry and 10 kg/s of fuel flow across each duct.

3. RESULTS

The results for the eight investigated cases are presented below. Table 2 summarizes the total pressure at the inlets (P_{in}), the temperature on the upper surface of the heat exchanger (T_{upper}), and the heat rate obtained from the area integration of the heat flux on the upper surface of the heat exchanger ($\dot{Q}_{fuel}$).

Table 2: Results of the simulation for the investigated cases.

Case	P_{in} [Pa]	T_{up} [K]	$\dot{Q}_{fuel}$ [W]
AOG-P-10	35,910	347.47	-14,342
AOG-S-10	8,680,700	348.34	-15,278
AOG-P-1	571	341.32	-12,678
AOG-S-1	134,475	345.22	-14,404
Cruise-P-10	35,910	288.71	-421,702
Cruise-S-10	8,680,700	304.32	-552,416
Cruise-P-1	571	244.08	-154,737
Cruise-S-1	134,475	253.38	-241,833

3.1 PRESSURE

From Table 2, it can be observed that cases which feature a serpentine configuration exhibit significantly higher P_{in} values compared to the cases with a parallel configuration. This difference is due to the combination of the small cross-sectional area of the ducts and the total length traveled by the fluid until it exits the heat exchanger in the serpentine configuration, where the sum of the individual duct lengths results in a total distance of over 220 meters.

The type of operation does not influence the pressure, as the boundary conditions for momentum conservation are identical among the cases, and the fuel properties are slightly impacted by the temperature levels found. As expected, the results are influenced by the mass flow rate, where higher $\dot{m}$ values result in higher P_{in}, and by the geometric configuration (duct length), as mentioned earlier.

3.2 TEMPERATURE

Evaluating the effect of the type of operation, it is notable that in cases where the operation is performed with the aircraft on the ground, the average temperature on the upper surface (T_{up}) exposed to the air-flow is very close to the inlet fuel temperature (T_{fuel}). This can be attributed to atmospheric conditions, as the air temperature is high and the wind speed is lower compared to cruise flight operations, resulting in lower heat exchanger efficiency.

For the cases where the operation occurs during cruise flight, a significant reduction in the average temperature on the upper surface was observed. This is due to the higher convection heat transfer driven by the fully turbulent external flow, and also favorable atmospheric conditions of low temperature for the air.

Analyzing the effect of geometry on the average temperature of the upper surface, the parallel geometry presents lower temperatures when compared to the serpentine configuration. This is due to the lower fuel mass flow in each duct, which promotes a greater temperature drop of the fuel, and, consequently, also reduces the average temperature surface. Finally, in cases where $\dot{m}$ is lower, it is noted that T_{up} also reduces. The lower mass flow rate improves the heat exchange due to the longer residence time of the fluid.

Figures 3 and 4 show the temperature at the outlet of each duct for the parallel configuration (T_{outlet}), and also at the end of each main section of the serpentine geometry cases ($T_{outlet*}$), which acts as the inlet temperature for the subsequent duct. The lowest temperature for the parallel configuration occurs at the first duct, which is the closest to the leading edge of the wing. On the other hand, the lowest temperature is recorded on the last duct (20) for the serpentine case, which is closer to the trailing edge.

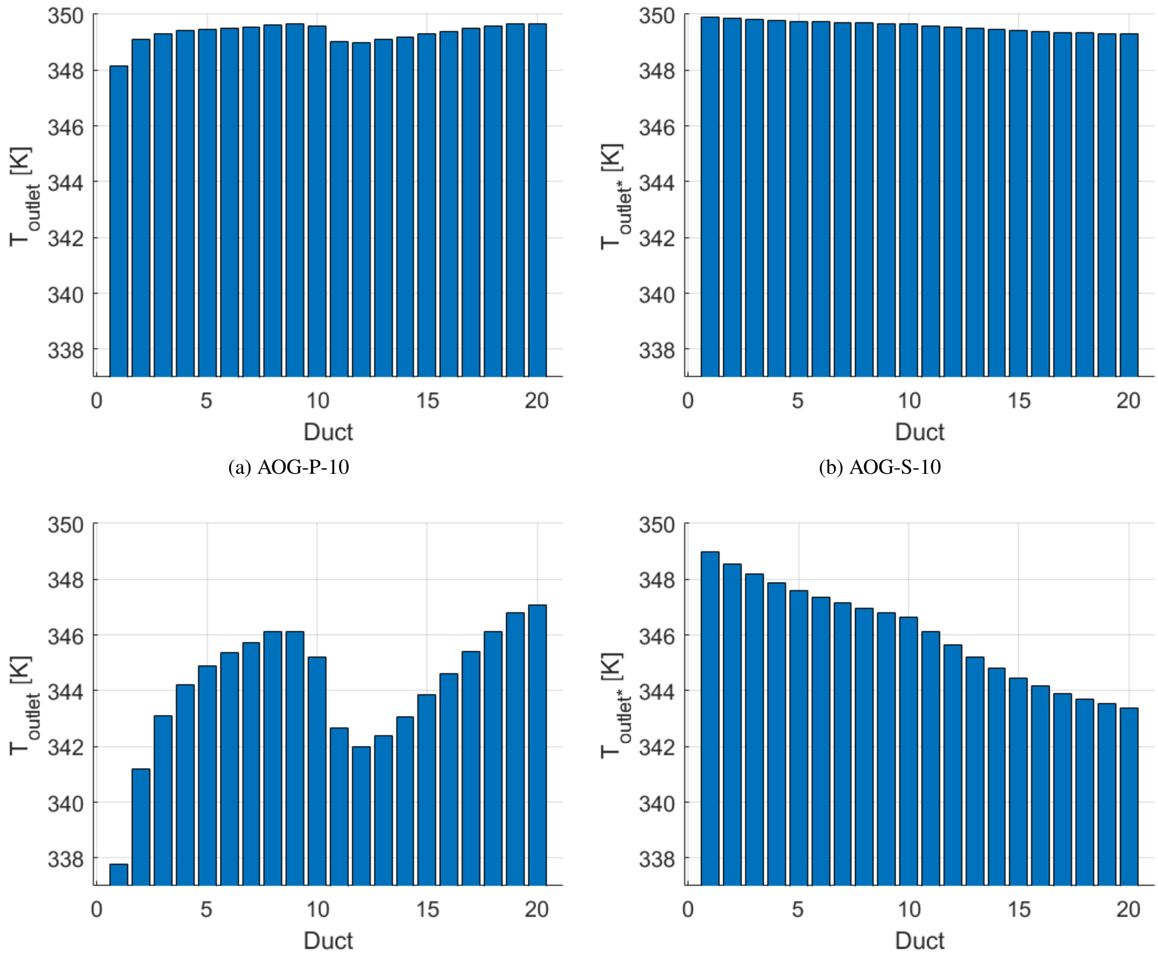

(a) AOG-P-10 (b) AOG-S-10

(c) AOG-P-1 (d) AOG-S-1

Figure 3: Outlet temperature of the ducts for AOG operation.

For AOG-P configurations there is a temperature decrease around the 10th duct due to the augmentation in the convective heat transfer coefficient, caused by the transition into turbulent regime. This also applies to AOG-S cases, resulting in a greater temperature decrease.

For the aircraft on the ground, the parallel geometry recorded the lowest temperature at the duct outlets. However, for the cruise flight scenario, the serpentine geometry resulted in the lowest temperature, but only when the mass flow was at its minimum.

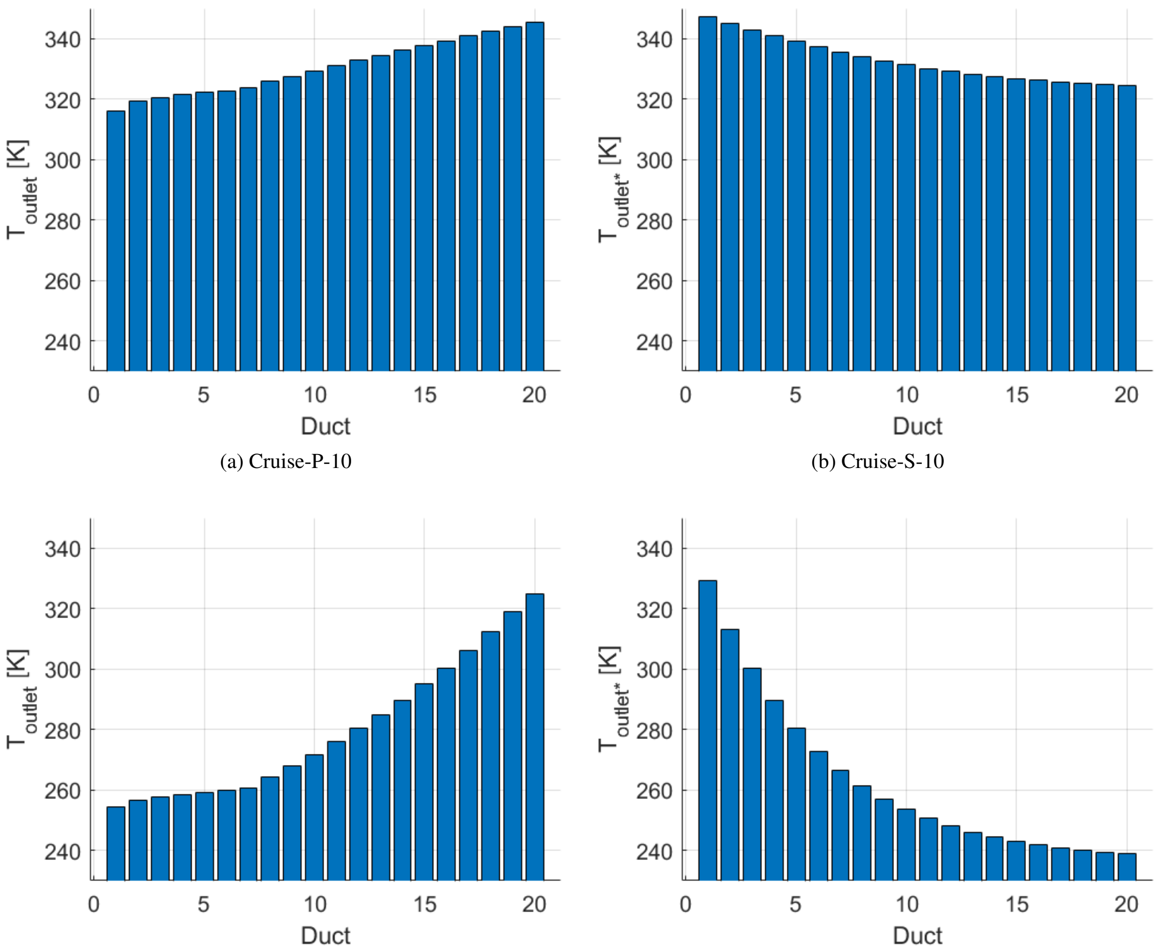

(a) Cruise-P-10

(b) Cruise-S-10

(c) Cruise-P-1

(d) Cruise-S-1

Figure 4: Outlet temperature of the ducts for cruise operation.

3.3 HEAT

Analyzing Table 2, $\dot{Q}_{fuel}$ is negative in all the cases, and represents the heat removal rate. The value of $\dot{Q}fuel$ is lower (in magnitude) in the cases where the aircraft is on the ground, indicating that less heat was exchanged during this type of operation. The value of $\dot{Q}fuel$ was significantly higher during cruise flight, as expected, with the cases featuring serpentine geometry and higher mass flow rates being more efficient in heat exchange. It is also notable that the reduction in mass flow rate during cruise flight resulted in a significant decrease in $\dot{Q}_{fuel}$. However, when the aircraft was on the ground, this decrease was not as pronounced.

Figures 5 and 6 display the heat flux on the upper surface of the heat exchanger. The scales for cases AOG are adjusted for easier visualization of the results compared to Cruise cases.

For all the cases AOG, the most intense heat flux is observed at the leading edge of the heat exchanger. This flux significantly decreases until the transition of the air flow from laminar to turbulent flow, where then increases again with turbulent flow. After the transition, the heat flux remains approximately constant up to the trailing edge of the heat exchanger.

Analyzing cases with Cruise, it is noticeable that the heat flux is more intense on the left side of the heat exchanger for the cases with parallel geometry and more intense at the leading edge for the cases with serpentine geometry. As the fuel exchanges heat with the flow, there is a decrease in it near the outlets. The less intense heat flux at the leading and trailing edges in all these cases results from the lower temperature of the upper surface and the absence of ducts in these regions.

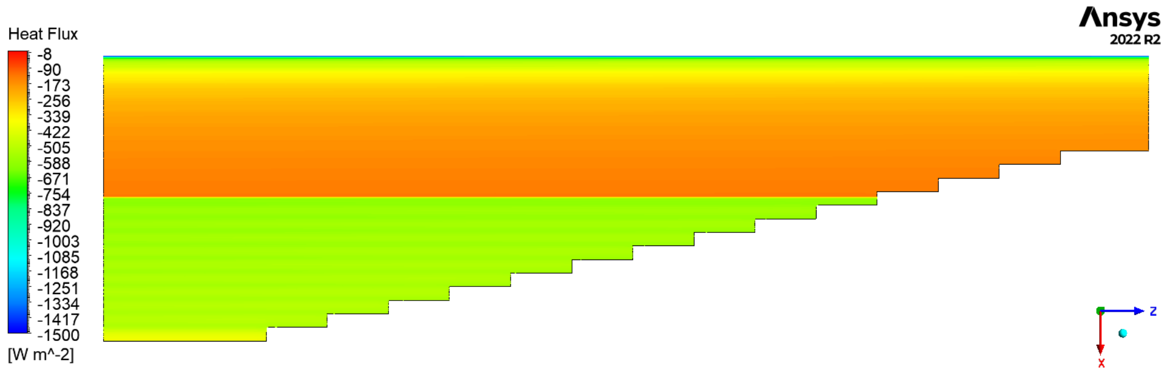

(a) AOG-P-10

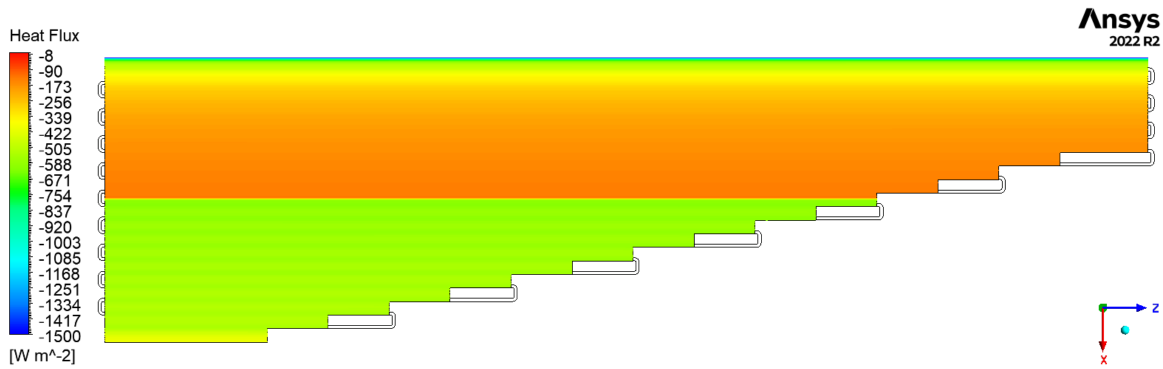

(b) AOG-S-10

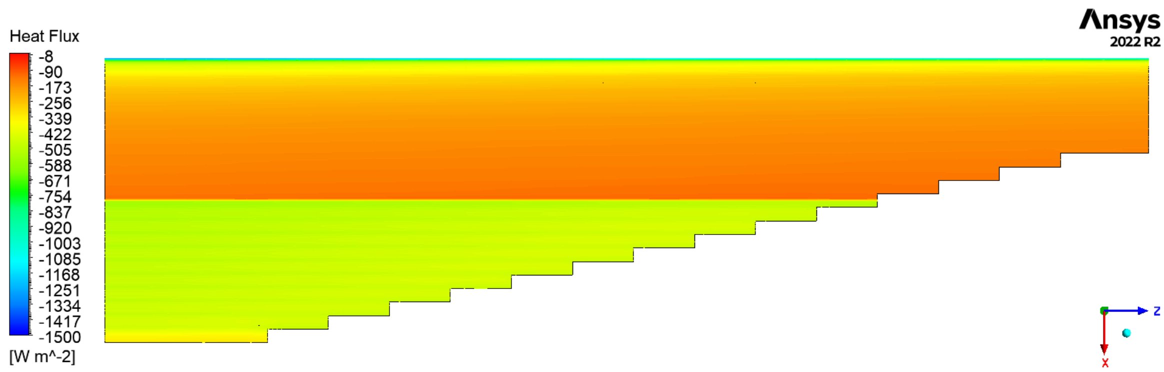

(c) AOG-P-1

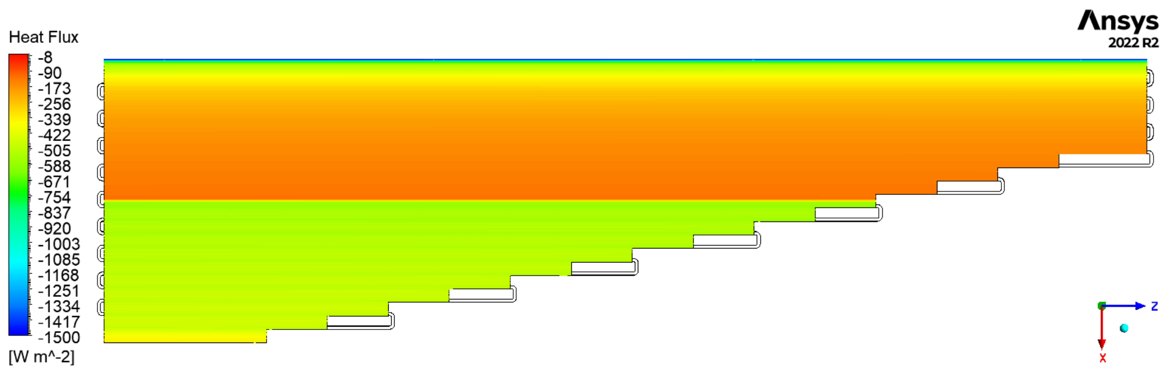

(d) AOG-S-1

Figure 5: Heat flux at the upper surface for cases AOG.

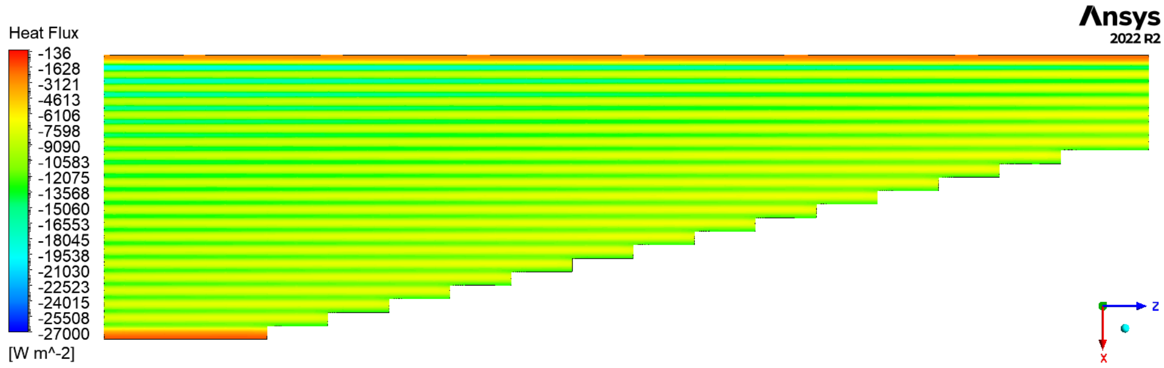

(a) Cruise-P-10

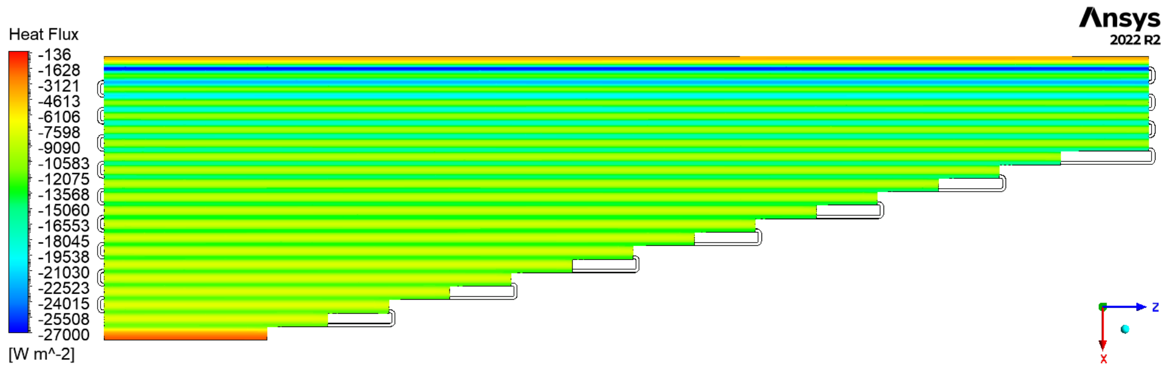

(b) Cruise-S-10

(c) Cruise-P-1

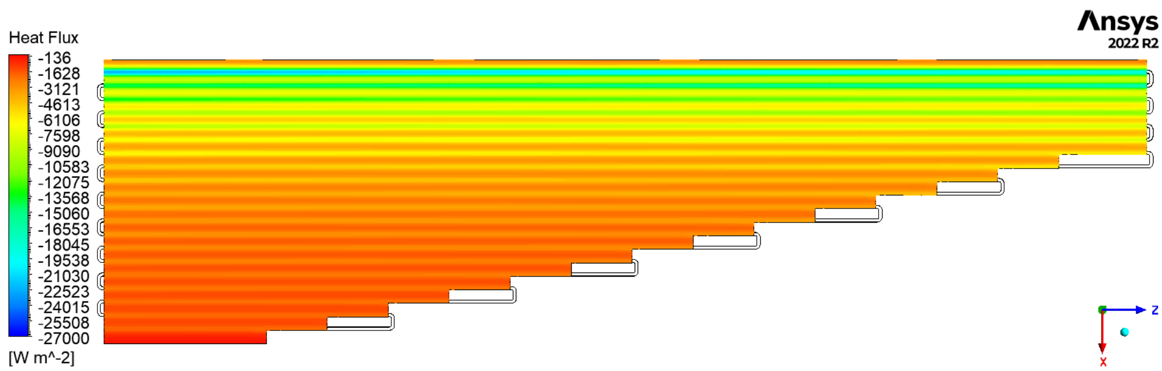

(d) Cruise-S-1

Figure 6: Heat flux at the upper surface for cases Cruise.

4. CONCLUSION

This study examined the use of fuel as a heat exchanger in commercial aircraft by modeling a heat exchanger based on the main tank of the Boeing 777-300ER and performing CFD simulations.

The results for the AOG cases indicated low values of $\dot{Q}_{fuel}$ (in magnitude) and high values of T_{up}, demonstrating low heat exchanger efficiency under these conditions. This inefficiency can be attributed to the higher ambient temperatures and lower wind speeds typical of ground operations, which reduce the overall heat transfer capability of the system.

For cases with serpentine geometry, $\dot{Q}_{fuel}$ was higher (in magnitude) compared to parallel configurations when operating under the same conditions and mass flow rates. However, the inlet pressure (P_{in}) was substantially higher in serpentine configurations, which may necessitate the installation of a more robust and heavier system in the aircraft. This trade-off between improved heat transfer and increased system complexity and weight needs to be carefully considered in the design phase.

Higher mass flow rates promoted greater heat exchange, but this also resulted in a smaller temperature drop of the fuel. This indicates that while increased flow rates enhance the heat transfer rate, they may not effectively cool the fuel due to reduced residence time within the heat exchanger.

The study highlights the importance of optimizing both the geometric configuration and operational parameters to achieve an efficient heat exchange system. Future work will include other types of analyses and simulations to further validate and compare the results obtained in this study. This will provide a broader understanding of the system's performance under varying conditions and help identify the most efficient configurations and operational strategies for fuel-based heat exchangers in aircraft.

5. ACKNOWLEDGEMENTS

The authors extend their sincere gratitude to São Paulo State University (UNESP) for funding this project (grant no. 10230), their support, and for providing the necessary software resources.

6. REFERENCES

Bruno, T.J., Huber, M., Laesecke, A., Lemmon, E., McLinden, M., Outcalt, S.L., Perkins, R., Smith, B.L. and Widegren, J.A., 2006. "Thermodynamic, transport and chemical properties of "reference" jp-8". *Book of Abstracts, Army Research Office and Air Force Office of Scientific Research*, pp. 15–18.

Ghajar, A. and Yunus A. Cengel, D., 2014. *Heat and Mass Transfer: Fundamentals and Applications*. McGraw-Hill Education. ISBN 9780073398181. URL https://books.google.com.br/books?id=B89MnwEACAAJ.

Gray, C. and Shayeson, M., 1973. "Aircraft fuel heat sink utilization. final technical report 14 apr 1972–14 apr 1973". Technical report, General Electric Co., Cincinnati, OH (USA). Aircraft Engine Technical Div.

Kellermann, H., Habermann, A., Vratny, P. and Hornung, M., 2020. "Assessment of fuel as alternative heat sink for future aircraft". *Applied Thermal Engineering*, Vol. 170, p. 114985.

Murad, J., 2020. "What is y+ (yplus)?" URL https://www.simscale.com/forum/t/what-is-y-yplus/82394.

Schwab, A., Thomas, A., Bennett, J., Robertson, E. and Cary, S., 2021. "Electrification of aircraft: Challenges, barriers, and potential impacts". doi:10.2172/1827628. URL https://www.osti.gov/biblio/1827628.

World Weather Online, 2024. "São paulo–guarulhos international airport (gru) annual weather averages". URL https://www.worldweatheronline.com/v2/weather-averages.aspx?q=gru. Access: April 12th, 2024.

7. RESPONSIBILITY NOTICE

The author(s) is (are) the only responsible for the printed material included in this paper.